

Analysis of Climate Change Projections for the Ministry of Transportation and Infrastructure Highways Risk Assessment

July 2014

**Stephen R. Sobie
Trevor Q. Murdock**



With support from Natural Resources Canada through the
Adaptation Platform



Natural Resources
Canada

Ressources naturelles
Canada

Canada

(Blank)

1. Citation

Sobie, S.R., Murdock, T.Q., 2014: *Analysis of climate change projections for the Ministry of Transportation and Infrastructure highway risk assessment*. Pacific Climate Impacts Consortium, University of Victoria, Victoria, BC, XX pp.

2. About PCIC

The Pacific Climate Impacts Consortium is a regional climate service centre at the University of Victoria that provides practical information on the physical impacts of climate variability and change in the Pacific and Yukon Region of Canada. PCIC operates in collaboration with climate researchers and regional stakeholders on projects driven by user needs. For more information see <http://pacificclimate.org>.

Disclaimer

This information has been obtained from a variety of sources and is provided as a public service by the Pacific Climate Impacts Consortium (PCIC). While reasonable efforts have been undertaken to assure its accuracy, it is provided by PCIC without any warranty or representation, express or implied, as to its accuracy or completeness. Any reliance you place upon the information contained within this document is your sole responsibility and strictly at your own risk. In no event will PCIC be liable for any loss or damage whatsoever, including without limitation, indirect or consequential loss or damage, arising from reliance upon the information within this document.

3. Acknowledgements

The authors are grateful to the British Columbia Ministry of Transportation and Infrastructure and to Natural Resources Canada for their support.

1. Introduction

This document is a supplementary report to the Ministry of Transportation and Infrastructure's comprehensive assessment concerning the risk of damage or failure due to climate change for three sections of highway in British Columbia (Nodelman, 2013). As part of the Public Infrastructure Engineering Vulnerability Committee (PIEVC) protocol (Lapp, 2013), the Pacific Climate Impacts Consortium (PCIC) analyzed and documented the impacts of climate change on precipitation at the different highway regions. The analysis involved historical observations, climate model simulations and tools such as statistical downscaling to project how precipitation averages and extreme events may change over the next 50 years.

The risk assessment process was coordinated through a series of meetings between MOTI staff and PCIC researchers. Collaboration for this assessment was done with the establishment of an MOTI working group, consisting of engineers, managers and staff from MOTI, consultants from Nodelcorp and scientists from PCIC. This risk assessment process culminated in a facilitated workshop involving the working group and other experts to review current vulnerabilities and assess future risk for specific infrastructure elements in the highway regions. Discussion of how the climate information was used in the risk assessment process, full descriptions of the three highway regions including the infrastructure components, and the results of the PIEVC process are documented within the risk assessment report. The information provided here is summarized within the report and was used to identify potential areas of concern on each of the three highway sections that could require changes to design specifications or maintenance practices.

2. Methods

2.1. Data

Initial climatological analysis of the three highway regions was conducted with weather station observations. The stations examined were obtained from the Provincial Climate Dataset (PCDS) created by PCIC. This dataset contains weather station observations from a variety of different observing networks throughout the province. All of the weather station data used in the analysis is publicly available through the PCDS Data Portal hosted on the PCIC website (www.pacificclimate.org).

At each of the three highway regions, we considered all available weather stations that satisfied a list of criteria for use in our analysis. Each station was required to have: observations of daily precipitation, thirty years of continuous observations, a location in close proximity to the highway, and few missing values in the record. Weather stations from Environment Canada were found to fulfill these criteria at the Bella Coola and Bear Pass sections, however none were available in the Pine Pass region. In that case, a single grid cell was taken from the ANUSPLIN gridded observational dataset (McKenney et al., 2011) to use in place of station observations. This dataset consists of 10km by 10km grid cells generated by interpolating weather station observations using a thin plate spline approach. The resulting data provides a uniform, gridded source of daily precipitation

observations for all of terrestrial Canada from 1951 to 2005 with no missing areas or missing values. For comparison, indicators computed from single ANUSPLIN grid cells are also compared to station values at Bella Coola and Bear Pass. The ANUSPLIN dataset was also used to calibrate the statistical downscaling method that was used to generate future projections.

Past and future simulations of climate were taken from a set of regional climate models (RCMs). RCMs operate in a similar fashion to global climate models, but at higher resolution and over a limited area (North America in this case). The RCMs used for this project were obtained from the North American Regional Climate Change Assessment Program (NARCCAP; Mearns et al., 2009). Ten available models possessed both historical (1971-2000) and future (2041-2070) simulations. We used daily precipitation over British Columbia from each of the regional climate models as input to statistical downscaling to further increase the spatial resolution to that of ANUSPLIN (10 km x 10 km), thus providing detailed climate information for each of the highway regions.

2.2. Downscaling Method

Statistical downscaling refers to a variety of methods that are used to relate coarse resolution climate model simulations to finer scales. The links between spatial scales are formed by identifying mathematical relationships between simulations from a climate model and observations for the same time period. One of the simplest versions of this is known as the 'delta method', which computes the difference between the 30-year average (or climatology) for a large-scale grid cell and the 30-year averages of all the small-scale grid cells located within the larger cell (Murdock & Spittlehouse, 2011). These differences are then applied to a future coarse scale simulation to produce a similar high-resolution output. This process effectively adds large-scale changes from the climate model to the local, high-resolution climatology.

As we are concerned with extreme precipitation events, a more sophisticated downscaling method is required. We used the Bias Correction/Climate Imprint (BCCI) downscaling technique (Hunter & Meentemeyer, 2005) to produce the fine scale climate model output. The method was selected based on an intercomparison of three different downscaling methods (Cannon, Sobie, & Murdock, In Prep). This technique is based on the delta method but employs additional steps to ensure that the entire precipitation distribution is adjusted from large to small scales, rather than just the average as is the case with the delta method. The BCCI technique first converts the daily values of both historical model output and observations to monthly climatologies. Then, it calculates anomalies of the model simulations relative to their monthly climatologies. These anomalies are interpolated to the resolution of the observations and 'imprinted' onto the observed climatology to produce high-resolution model output. The final step is to apply a de-trended bias correction to the precipitation values at each grid cell. This ensures that the occurrence of extreme events more closely matches those of the observations at each cell. We produced high-resolution simulations of past and future climate by applying this statistical downscaling technique to ten regional climate models.

2.3. Climate Indicators

The indicators were developed based on previous highway risk assessments (e.g. Nodelman, 2010) and in discussion with the MOTI working group. The parameters were chosen to represent different types of weather events that have or could lead to significant infrastructure impacts. All but one of the indicators was derived from daily precipitation. The values included long-term averages such as annual total precipitation, multi-day precipitation totals and extreme events such as 10 and 25-year return period amounts. Return periods were calculated from annual precipitation maxima with the R-Packages "ismev" and "extRemes" using maximum likelihood estimation to fit a Generalized Extreme Value (GEV) probability distribution to the data (Zwiers et al., 2013). As snowfall was not available from either the downscaled output or the ANUSPLIN dataset, a snowfall proxy was used instead, computed from the daily total precipitation that occurred when the daily minimum temperature was below zero. The number of days where the snow proxy exceeded 10 mm was computed, following a snow days indicator from a previous PIEVC risk assessment (Nodelman, 2010).

Certain parameters included in the current risk assessment covering the three highway regions were not examined using the downscaled climate model data (e.g. ice jams, debris flows) either due to insufficient data availability or because the data required could not be computed directly from the available downscaled variables (daily minimum temperature, daily maximum temperature, and daily precipitation). For example, snowmelt driven peak streamflow was identified as having caused significant damage to infrastructure in past and therefore would be of interest to engineers and highway maintenance workers. These types of additional parameters were included in the assessment at the request of the MOTI working group due to the higher vulnerabilities associated with the more complex indicators. These other parameters were addressed separately following the PEIVC risk assessment protocols (Lapp, 2013).

3. Highway Regions

3.1. Bella Coola Highway

The Bella Coola highway is located in the western part of British Columbia within the Coast Mountain range at the end of a coastal fjord (Figure 1). The highway links Bella Coola with the interior of the province and extends east from the coastal, mountainous geography of Bella Coola to the interior plateau of Tatla Lake. As a result, the highway passes through two distinct climate regimes, a more maritime climate in the western half of the region and a more continental climate to the east. Precipitation on the highway occurs primarily during the autumn and winter months, with the largest amounts occurring in November, December (Figure 2). A (smaller) peak during the summer months indicates the effect of convective events predominantly in the eastern half of the region (Moore, Spittlehouse, Whitfield, & Stahl, 2010).

Winter precipitation is dominated by synoptic scale storms from the northern Pacific. Many of the largest winter precipitation events are associated with Atmospheric Rivers

which transport significant quantities of water vapour from the ocean onto the coast (Dettinger, Ralph, Das, Neiman, & Cayan, 2011). Interaction between this prevailing westerly flow from the Pacific Ocean and the Coast Mountains results in substantial orographically generated precipitation on the windward slopes, particularly in the western half of the highway region. Steep topography surrounding the highway funnels runoff from precipitation into the Bella Coola River, which runs parallel to the highway along its western sections.

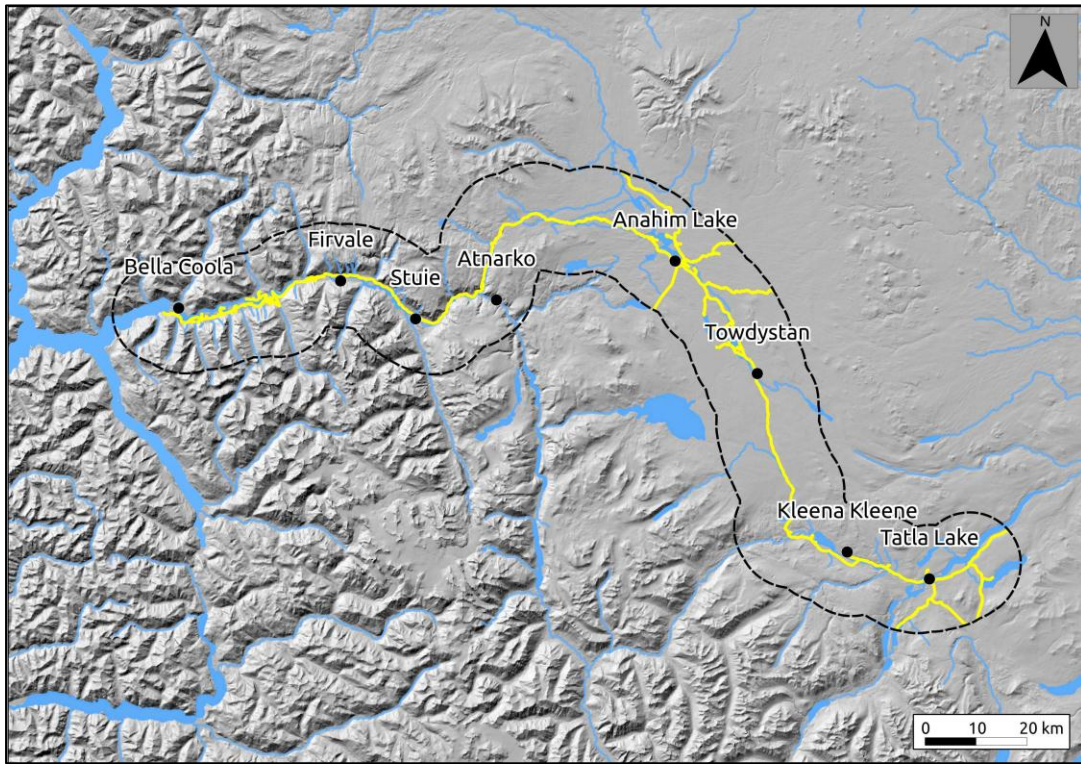


Figure 1: Topographic map of the Bella Coola Highway section from Bella Coola to Tatla Lake. The yellow line shows the path of Highway 20 to Bella Coola. The dashed line shows the area within 10 km of the highway including many of the waterways, hillsides and slopes that intersect the road.

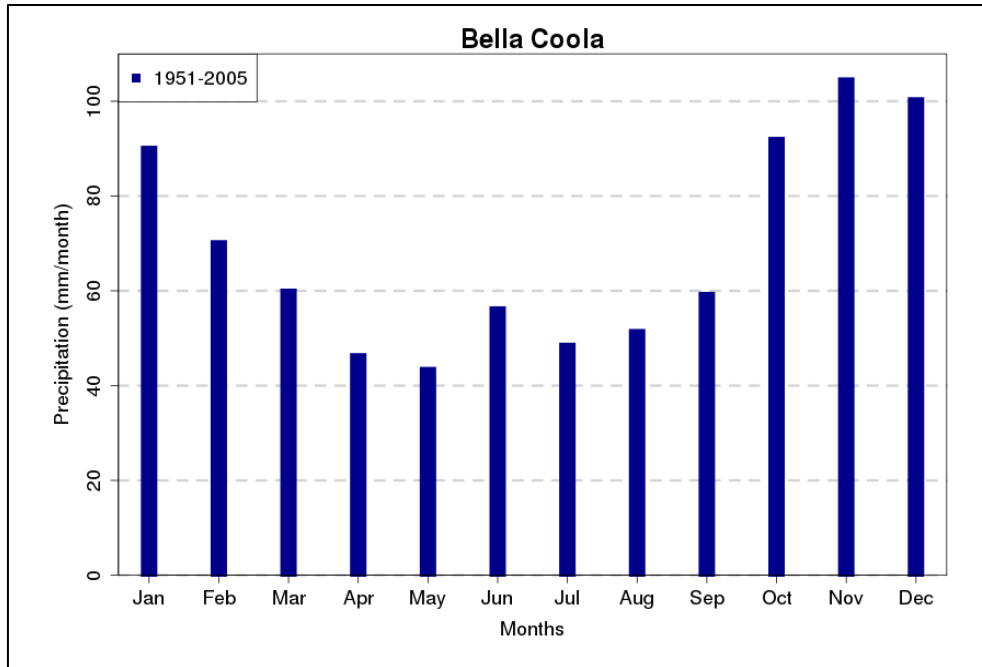


Figure 2: Monthly precipitation totals for Bella Coola Highway obtained from the ANUSPLIN dataset and averaged over 1951-2005. The values are computed from regional averages of the observations located within the 10 km boundary surrounding the highway.

3.2. Bear Pass Highway

The Bear Pass highway is located in the north-western part of British Columbia near the southern tip of the Alaskan Panhandle. The roadway runs from the city of Stewart at the northern end of the Portland Canal (a coastal fjord) to Meziadin Junction further inland. It is similar in location and climate to the Bella Coola region but receives a larger amount of precipitation annually. Monthly precipitation follows a typical coastally influenced pattern, with the lowest amounts occurring during summer and the highest during winter, predominantly as snow. The highway's proximity to the Gulf of Alaska and the Aleutian Low results in the region receiving precipitation from synoptic scale storms more frequently than the other regions, especially during the spring and fall. As with Bella Coola, the highway lies in an area of steep topography and follows parallel to a river (the Nass).

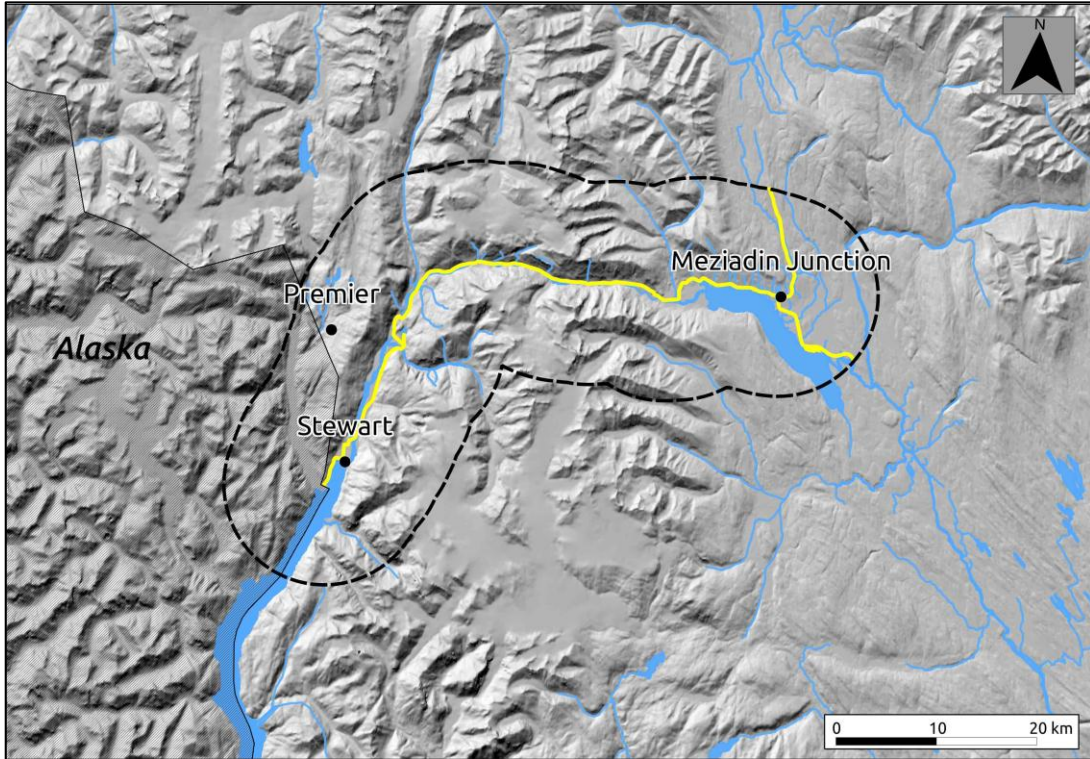


Figure 3: Topographic map of the Bear Pass Highway section from Stewart to Meziadin Junction. The yellow line shows the path of Highway 37A to Stewart. The dashed line shows the area within 10 km of the highway including many of the waterways that intersect with the road.

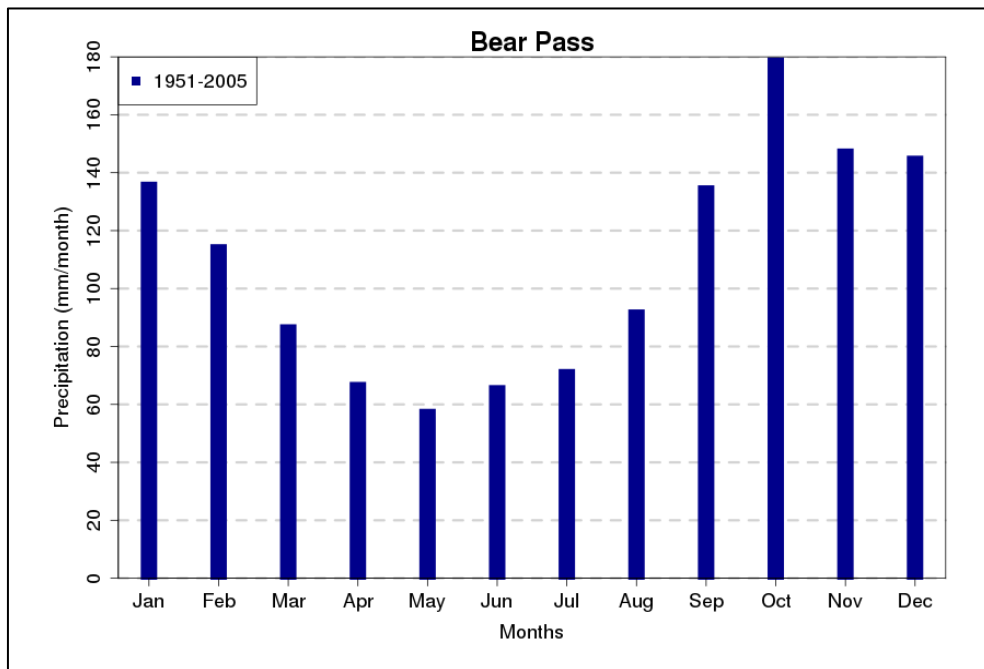


Figure 4: Monthly precipitation totals for Bear Pass Highway obtained from the ANUSPLIN dataset and averaged over 1951-2005. The values are computed from regional averages of the observations located within the 10 km boundary surrounding the highway.

3.3. Pine Pass Highway

The Pine Pass highway is located in the north-eastern part of British Columbia within the northern reaches of the Rocky Mountains. The highway runs between Mackenzie and Chetwynd and follows the route of the Pine River. Given the region's northern latitude, high elevation and distance from the coast, this highway experiences the coldest conditions of any of the regions. The region exists in a much more continental precipitation regime than the other two highway sections due to its inland location. This is reflected in the area's monthly precipitation distribution, which shows the highest precipitation amounts occurring during the summer, primarily due to convective activity (Moore et al., 2010). Past extreme precipitation events are often compounded in their severity by the nature of the terrain in the Pass and by the construction of the highway infrastructure, which tends to be older and more susceptible to damage from debris (Nodelman, 2013).

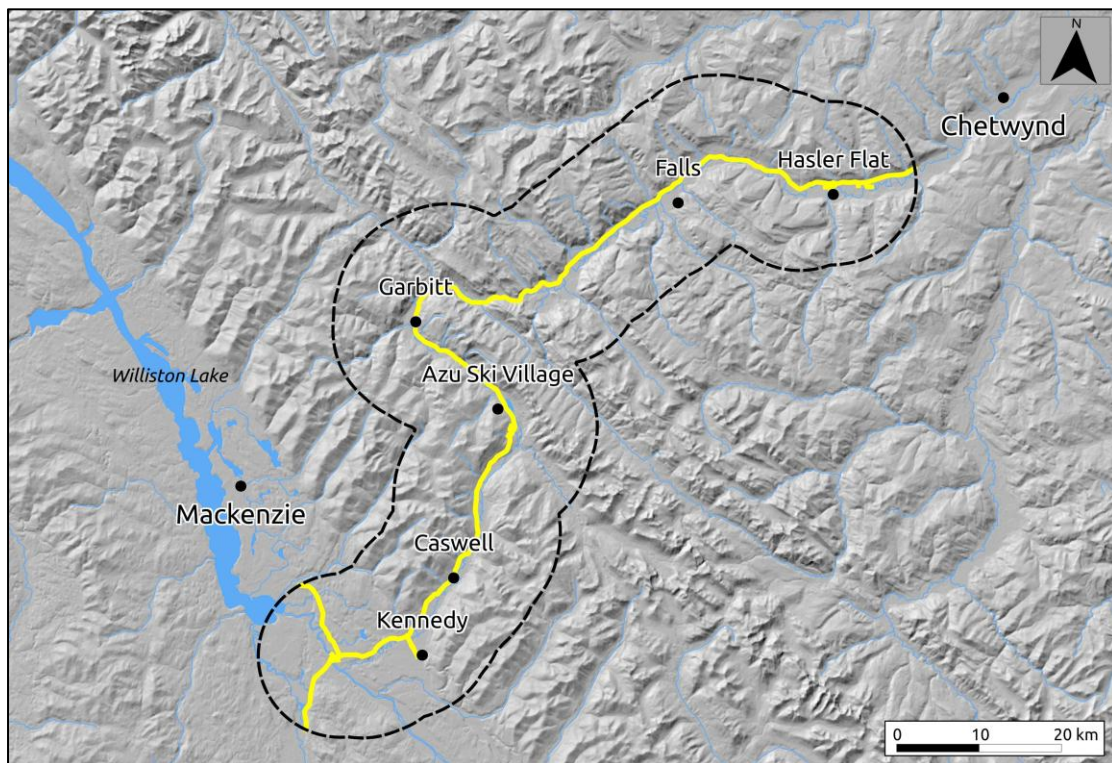


Figure 5: Topographic map of the Pine Pass Highway section from Mackenzie to Chetwynd. The yellow line shows the path of Highway 97. The dashed line shows the area within 10 km of the highway including many of the waterways that intersect with the road.

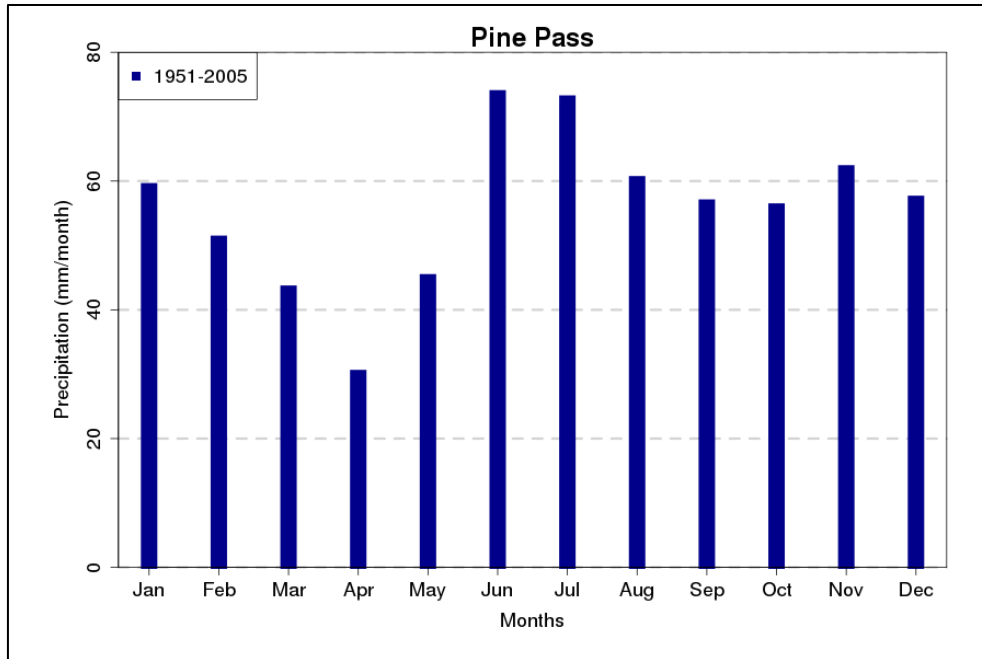


Figure 6: Monthly precipitation totals for Pine Pass Highway obtained from the ANUSPLIN dataset and averaged over 1951-2005. The values are computed from regional averages of the observations located within the 10 km boundary surrounding the highway.

4. Results

In each of the three highway sections, indicators are calculated from weather station observations, a single ANUSPLIN grid cell, averages of all ANUSPLIN observations within the region, and averages of downscaled models within the region. The different types of historical quantities are presented to distinguish between station, single site and regional observations. Station observations represent the weather at a single site. Gridded observations such as ANUSPLIN have uniform values within each grid cell, and cover more area than is captured by a station. As precipitation intensities can vary strongly over short distances, the quantities observed by a single point (weather station) can differ from those observed at a single 10 km x 10 km grid cell. To illustrate this difference, at Bella Coola and Bear Pass highway regions, indicators are computed from both a weather station and from the ANUSPLIN grid cell within which the weather station resides. Furthermore, the highway regions are defined as an area within 10 km of the highway, denoted by the dashed lines in Figures Figure 1Figure 3Figure 5. The boundaries are designed to encompass both the highway and any slopes, streams or other topographic features that could affect the road. These regions consist of 191, 74, and 116 grid cells for Bella Coola, Bear Pass, and Pine Pass, respectively.

Highway indicators have been assessed for each of the three regions including past and future climatologies, and future change as both absolute and percent anomalies. The five indicators presented include annual total precipitation, annual maximum 5-day precipitation total, 10-Year and 25-Year return periods for single day precipitation

amounts, and a snowfall proxy. Regional averages are calculated by first computing the indicator at each of observed or modelled grid cells and then taking a spatial average. Maps of past climatologies and projected future change are also included to illustrate the spatial variability at each of the three highway regions.

When presenting results from the ten downscaled climate model simulations, three values are given: the maximum value, the minimum value, and the average of all ten models (known as the ensemble average). This is done to illustrate the range in projections obtained by using multiple climate models. The variation between model simulations may be due to differences in the regional climate models and their driving global models, and from simulated climate variability over the 2041-2070 period. They may not be attributed to differences in emissions as all runs follow the SRES A2 emissions scenario (Nakićenović, 2000).

Increases are projected in all three regions in both average and extreme precipitation, though the magnitudes of change are different at each site. The more extreme events, notably the return periods, tend to display the largest ranges among the models. This arises due to uncertainties in fitting the GEV to finite (30-year) datasets and differences in how each of the models' simulated precipitation is adjusted by the downscaling process. While longer simulations from GCMs could provide more input to calculating the return period values, moving to parameters of rare extremes, such as higher return period values, also comes with greater uncertainty in the parameters themselves. Averaging the results from 10 different models helps to reduce this uncertainty but also introduces uncertainty from using multiple models. The combined effects from these different sources of uncertainty can be seen in the ranges of the projected changes, which increase from a relatively narrow spread in the total annual precipitation to the much larger spread in the 25-year return period (Tables Table 2Table 4Table 6).

4.1. Bella Coola

The weather station used for the Bella Coola section (Bella Coola Station) is located at the western edge of the highway, in the town of Bella Coola (Figure 7). This site receives nearly 1500 mm annually based on 107 years of observations from 1895 to 2002 (**Error! Reference source not found.**). Historical winter and summer climatologies (1951-2005) from ANUSPLIN observations (Figure 7) show that western part of the region receives more precipitation during the winter months than the rest of the highway section while precipitation is more uniformly distributed along the highway during the summer season. The regional average annual total for the entire highway section (within the 10km dashed boundary) is at 673 mm/year (**Error! Reference source not found.**).

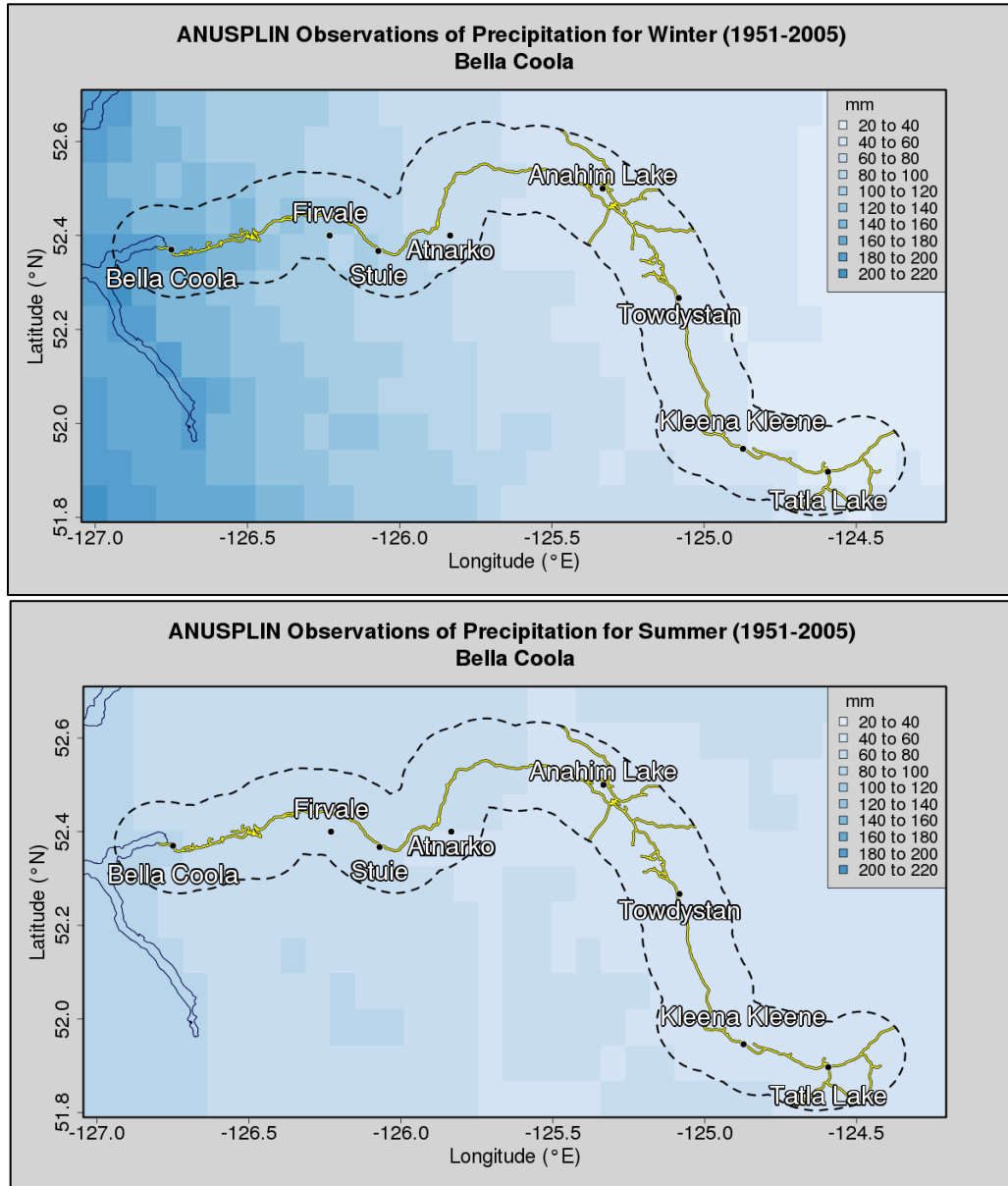


Figure 7: Winter (top) and summer (bottom) seasonal precipitation totals for the Bella Coola Highway (yellow line) obtained from the ANUSPLIN gridded observations and averaged over 1951-2005. Station indicators are computed from the Bella Coola weather station (located at Bella Coola). The regional indicators are computed from regional averages of the observations located within the 10 km boundary surrounding the highway (dashed line).

Comparing the individual site values to the regional extremes, the 10-Year and 25-Year 1-day return period values are about three times higher when calculated at the station than when computed from the ANUSPLIN regional average (**Error! Reference source not found.**). Similarly, longer duration precipitation as represented by the annual maximum 5-day total precipitation amount is 150 mm at the station and 56 mm over the region. For comparison, the 2010 storm that resulted in substantial flooding was a four-day event with 262 mm of precipitation at Bella Coola station.

Indicator	Station Value	ANUSPLIN Cell Value	ANUSPLIN Regional Value
Annual Total Precipitation (mm/year)	1456	1514	673
5-Day Total Precipitation (mm)	150	55	56
10-Year Return Period (mm/24 hrs)	105	72	36
25-Year Return Period (mm/24 hrs)	127	83	44
Snow Proxy (events/year)	14	22	6

Table 1: Precipitation indicators for Bella Coola highway from weather station (1895-2002) and ANUSPLIN (1951-2005) observations. The ANUSPLIN Cell indicators are calculated for the grid cell containing the weather station. The regionally averaged values are obtained from the spatial average of the cells within the 10km highway region boundary.

Maps of future precipitation are provided for both absolute (mm) and relative (%) changes in Figures Figure 8 and Figure 9 to demonstrate how small changes in precipitation amount can result in large relative change when the historical precipitation climatology is small. Absolute changes from the ten downscaled model projections (Figure 8) show increases in winter with the largest increases in the western half of the region, and little to no changes projected for summer. In contrast, when expressed as percent change relative to historical baseline (Figure 9), increases are largest in the eastern half reflecting the lower historical amounts in this part of the highway area.

The maps in Figure 8 Figure 9 are ensemble averages of ten different regional climate model simulations. Individual projections that make up these maps differ, as shown in Figure 10 for the regional average precipitation change. Although some models indicate considerably wetter futures than others, the majority of the models project increased precipitation in winter. This is also true for each of the other indicators listed in **Error! Reference source not found.**

Error! Reference source not found. indicates that extreme events are projected to increase by larger amounts than annual precipitation. In general, the less frequent the occurrence of events represented by an indicator, the larger the relative change. For example, while total annual precipitation is projected to increase by 11% in the 2050s compared with 1971-2000, the corresponding increases in annually averaged, monthly 5-day precipitation maxima and 25-year 1-day return period events are 20% and 36%, respectively. By the 2050s, the projected change in snow proxy value shows a 12% increase. As climate also warms by this time, this could result in an increased potential for rain on snow events and changes to snowpack levels. However, the snow indicator is a proxy only and rain on snow events were not analyzed directly.

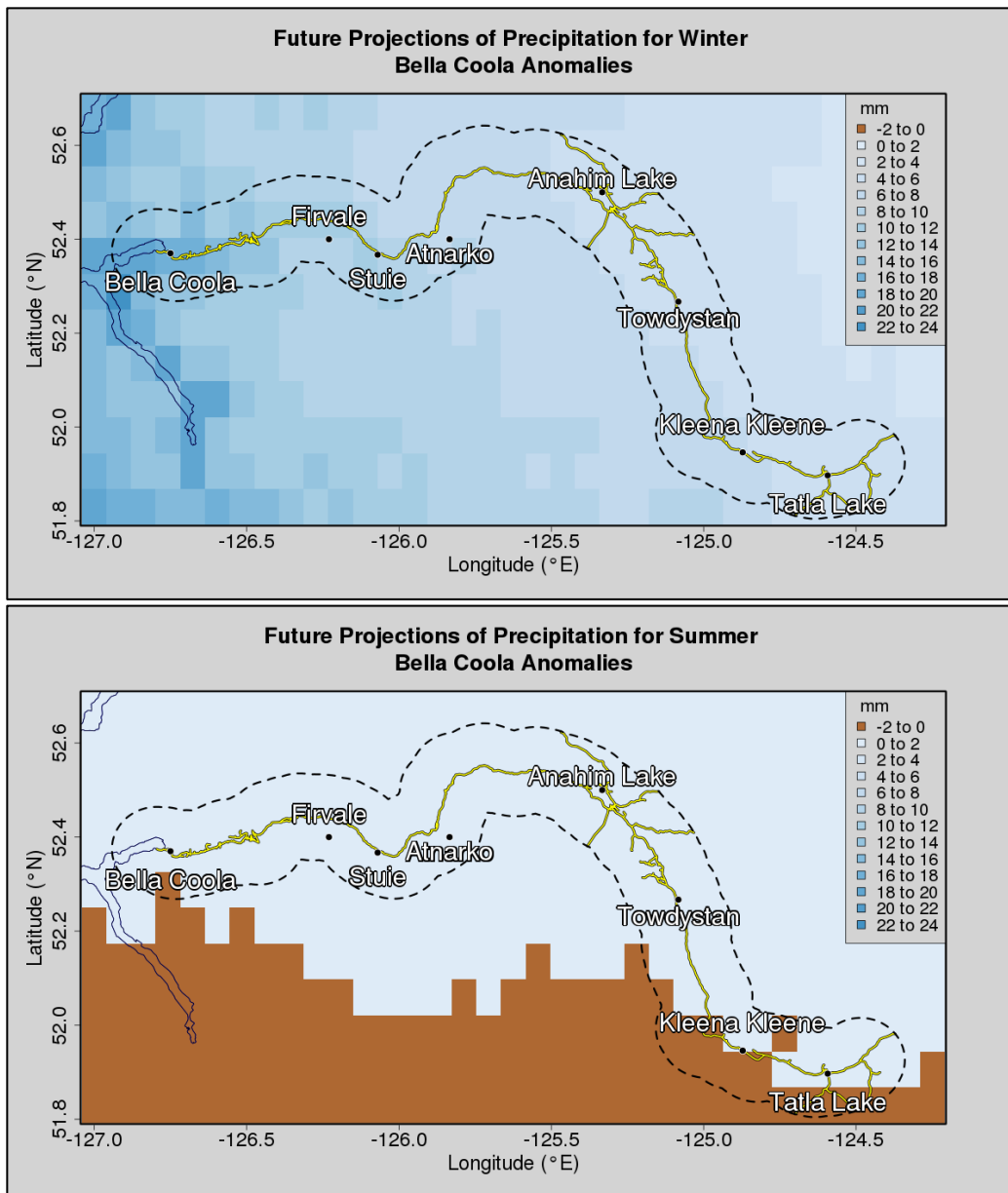


Figure 8: Projected 2050s absolute anomalies of winter (top) and summer (bottom) seasonal precipitation totals for the Bella Coola Highway (yellow line) obtained from an ensemble of 10 downscaled regional climate models. The regional indicators are computed from averages of the grid boxes located within the 10 km boundary surrounding the highway (dashed line).

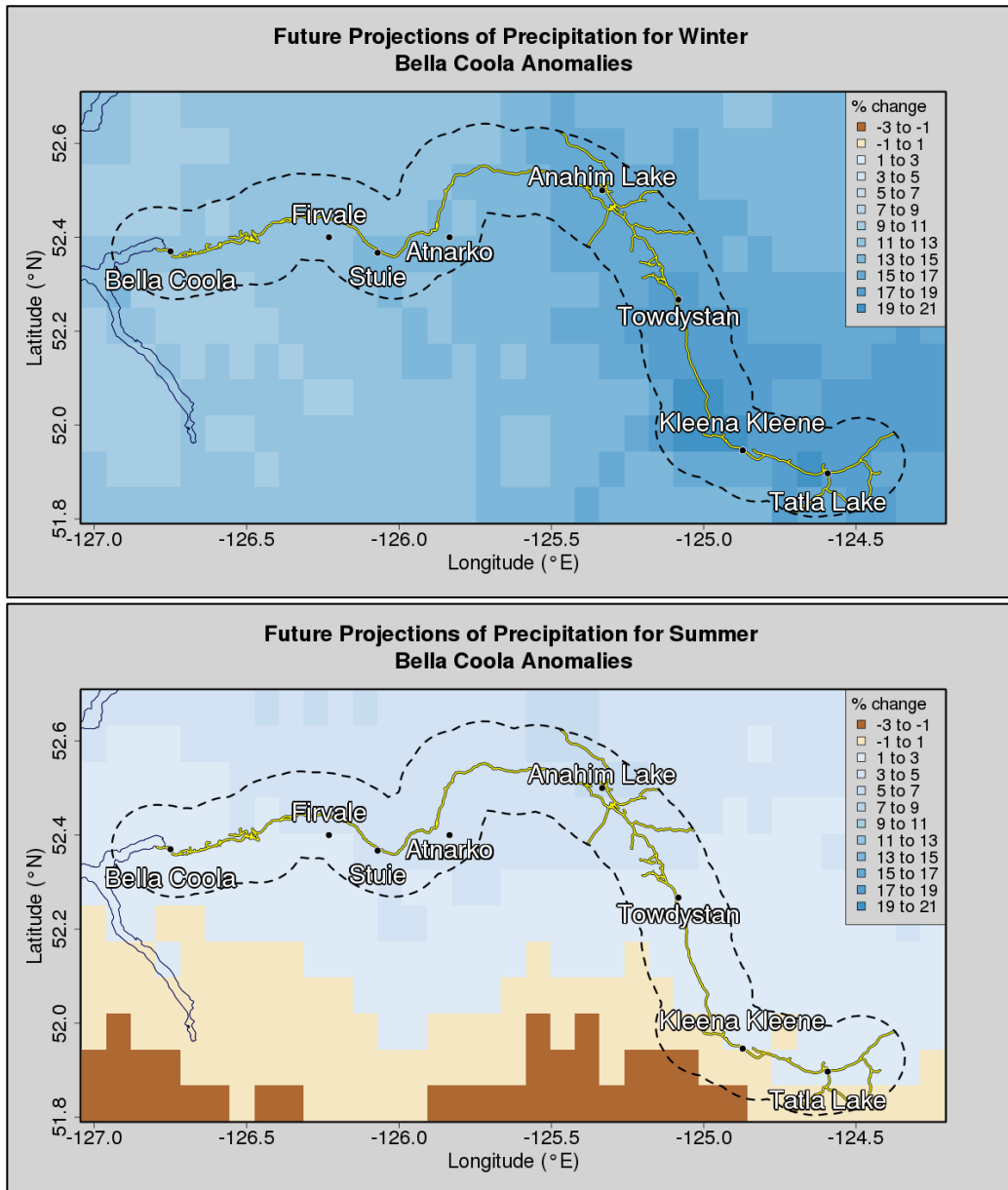


Figure 9: Projected 2050s (percent change) in winter (top) and summer (bottom) precipitation for the Bella Coola Highway (yellow line) obtained from an ensemble of 10 downscaled regional climate model simulations. The regional indicators are computed from averages of the grid cells located within the 10 km boundary surrounding the highway (dashed line).

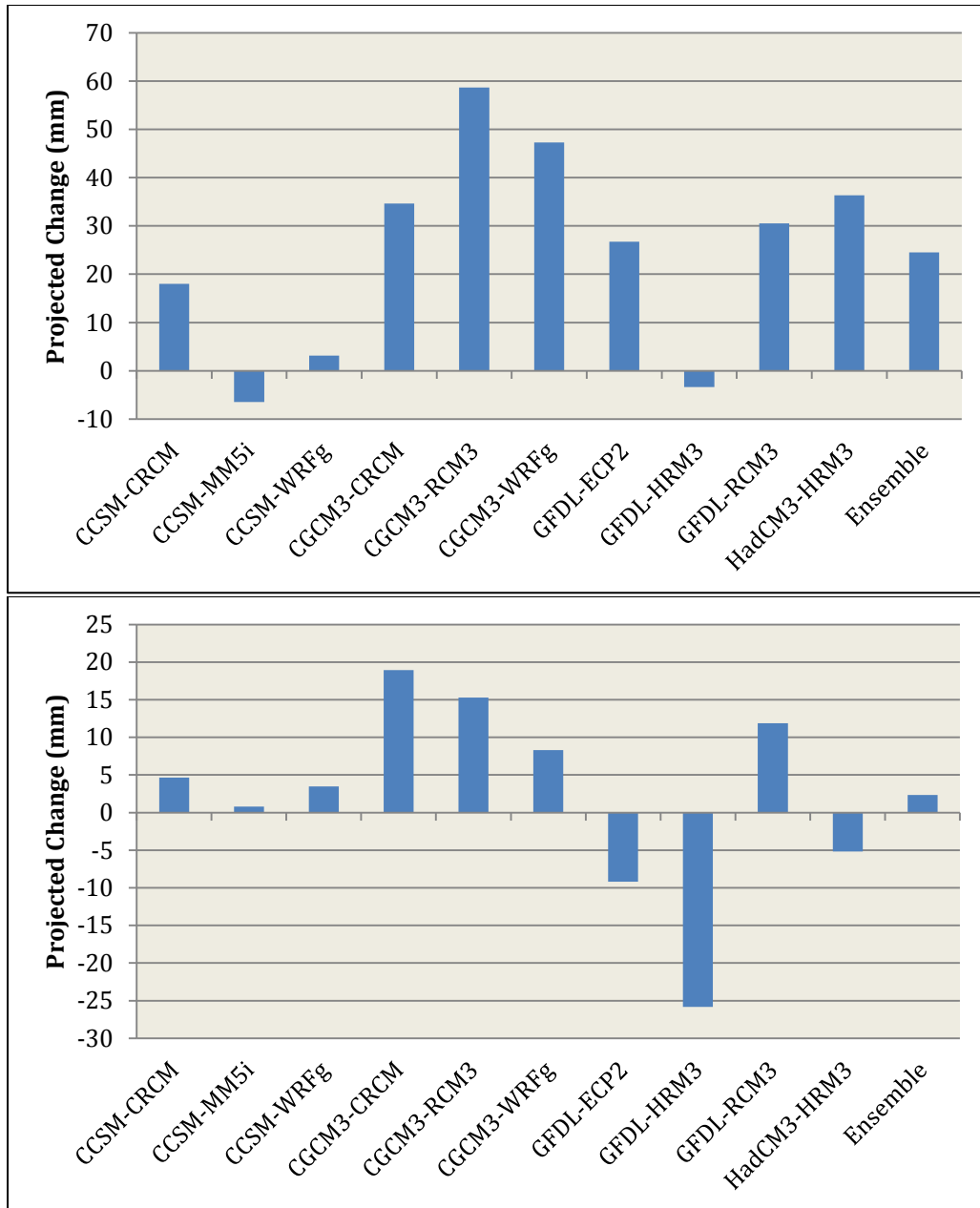


Figure 10: Projected 2050s anomalies of winter (top) and summer (bottom) precipitation totals for the Bella Coola Highway obtained from an ensemble of 10 downscaled regional climate models. The indicators are computed from regional averages of the observations located within the 10 km boundary surrounding the highway.

Annual Total Precipitation (mm/year)	Ensemble Average	Range (Min to Max)
Past (1971-2000)	673	664 to 677
Future (2041-2070)	744	641 to 807
Absolute Anomalies (mm)	71	-32 to 130
Percent Anomalies (%)	11	-5 to 19
5-Day Precipitation (mm)	Ensemble Average	Range (Min to Max)
Past (1971-2000)	56	53 to 60
Future (2041-2070)	67	57 to 75
Absolute Anomalies (mm)	10	-1 to 18
Percent Anomalies (%)	20	-2 to 32
10-Year Return Period (mm)	Ensemble Average	Range (Min to Max)
Past (1971-2000)	36	33 to 38
Future (2041-2070)	47	36 to 58
Absolute Anomalies (mm)	11	-2 to 23
Percent Anomalies (%)	31	-5 to 68
25-Year Return Period (mm)	Ensemble Average	Range (Min to Max)
Past (1971-2000)	44	39 to 53
Future (2041-2070)	60	45 to 77
Absolute Anomalies (mm)	16	-4 to 32
Percent Anomalies (%)	36	-9 to 79
Snow Proxy (events)	Ensemble Average	Range (Min to Max)
Past (1971-2000)	6.2	5.5 to 6.8
Future (2041-2070)	6.9	5.3 to 8.1
Absolute Anomalies (events)	0.8	-0.1 to 1.8
Percent Anomalies (%)	12	-3 to 30

Table 2: Projections of precipitation indicators from 10 downscaled regional climate model simulations for Bella Coola Highway. The regionally averaged values are obtained from the spatial average of the cells within the 10km highway region boundary.

4.2. Bear Pass

Projected changes in Bear Pass precipitation are similar to those of Bella Coola in relative size, though the overall conditions are wetter and the projected absolute changes larger in this area. The smaller area and more homogeneous climatology of this highway section results in closer agreement between the regionally averaged values from gridded data and values at the station. In this region the representative station is Stewart Airport with records spanning the years 1974-2011. Annually averaged total precipitation at Stewart is 1802 mm, the average 5-day total precipitation is 164 mm and the more return periods exceed 100 mm in 24 hours. In comparison, the regionally averaged gridded observations report amounts that are about two-thirds the size of those observed at the station and the single cell values are in between these two quantities (**Error! Reference source not found.**). Historical precipitation is distributed evenly throughout the highway section during the summer months while during the winter, the area in and around Stewart experiences greater precipitation than the rest of the highway (Figure 11).

Indicator	Station Value	ANUSPLIN Cell Value	ANUSPLIN Regional Value
Annual Total Precipitation (mm/year)	1802	1530	1290
5-Day Total Precipitation (mm)	164	54	96
10-Year Return Period (mm/24 hrs)	103	71	64
25-Year Return Period (mm/24 hrs)	116	84	75
Snow Proxy (events/year)	15	26	18

Table 3: Precipitation indicators for Bear Pass highway from weather station (1974-2011) and regionally averaged ANUSPLIN (1951-2005) observations. The ANUSPLIN Cell indicators are calculated for the grid cell containing the weather station. The regionally averaged values are obtained from the spatial average of the cells within the 10km highway region boundary.

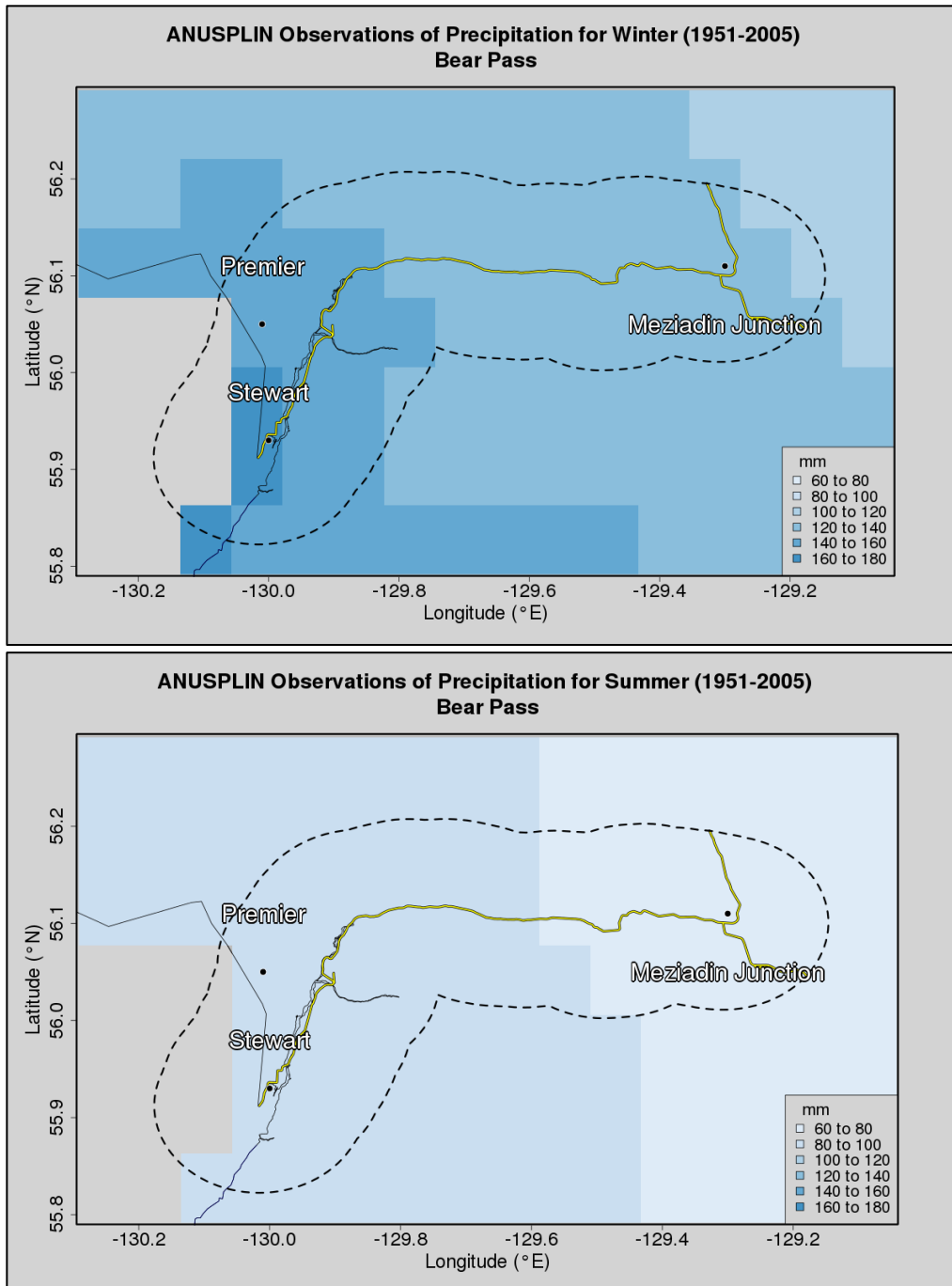


Figure 11: Winter (top) and summer (bottom) precipitation totals for the Bear Pass Highway (yellow line) obtained from the ANUSPLIN dataset and averaged over 1951-2005. The dashed line indicates the 10km highway region boundary.

Projected changes in future precipitation are mostly increases, with decreases only for the month of July at some locations. As with Bella Coala, the largest projected increases in precipitation are during the months of October through February. In Bear Pass, the absolute projected increases in all seasons are tend to be largest at the western end of the

highway near Stewart, though the relative increases are quite uniform throughout the region (Figure 12). Annual total precipitation is projected to increase by 14% over the region. All of 5-day total, 10-year 1-day return period precipitation and snow proxy amounts are projected to increase by 25% in the 2050s relative to the past (**Error! Reference source not found.**). The projections indicate relative changes for the Bear Pass highway that are similar to those for the Bella Coola highway.

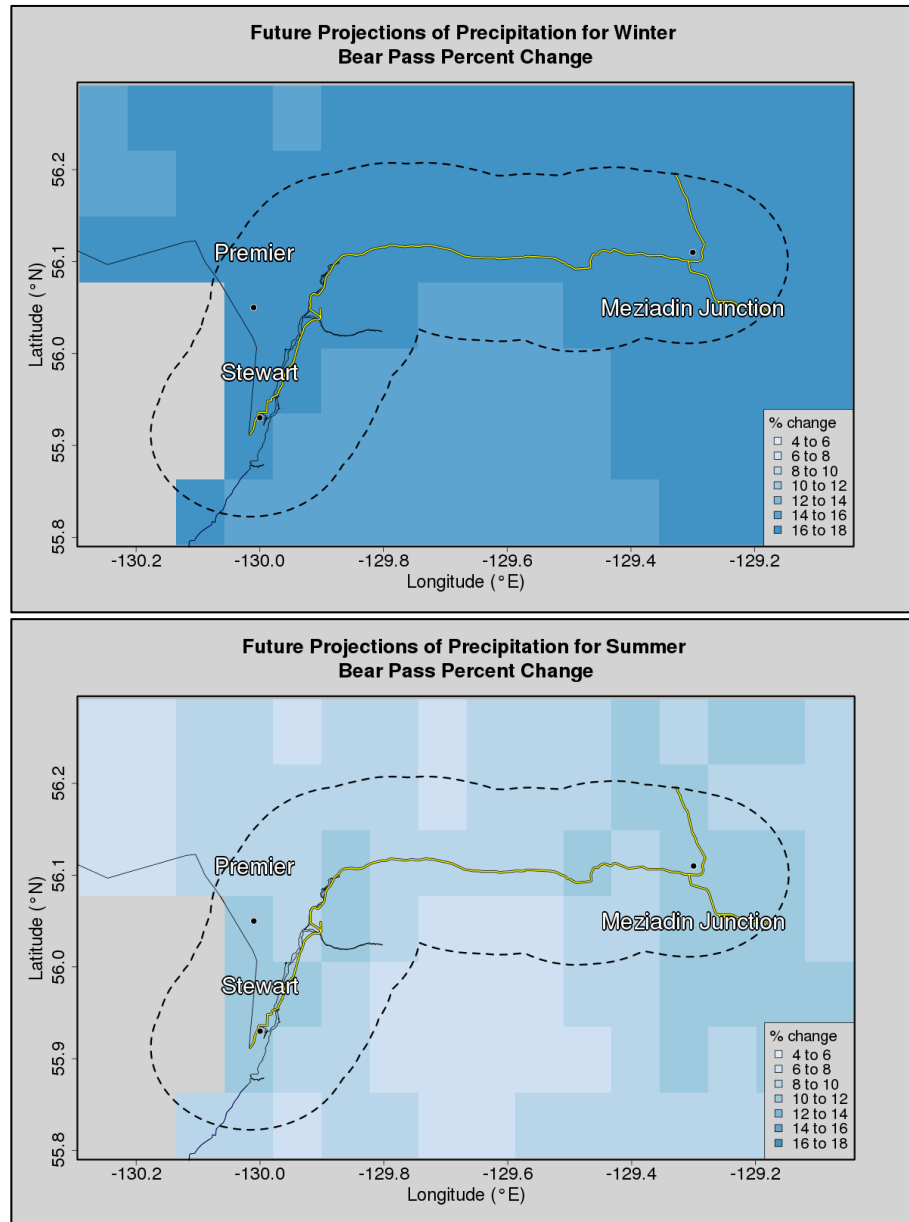


Figure 12: Projected 2050s (percent change) in winter (top) and summer (bottom) precipitation for the Bear Pass Highway (yellow line) obtained from an ensemble of 10 downscaled regional climate model simulations. The dashed line indicates the 10km highway region boundary.

Annual Total Precipitation (mm/year)	Ensemble Average	Range (Min to Max)
Past (1971-2000)	1290	1274 to 1310
Future (2041-2070)	1477	1344 to 1606
Absolute Anomalies (mm)	187	52 to 296
Percent Anomalies (%)	15	4 to 23
5-Day Precipitation (mm)	Ensemble Average	Range (Min to Max)
Past (1971-2000)	96	89 to 101
Future (2041-2070)	120	112 to 134
Absolute Anomalies (mm)	24	14 to 37
Percent Anomalies (%)	25	14 to 38
10-Year Return Period (mm)	Ensemble Average	Range (Min to Max)
Past (1971-2000)	64	62 to 66
Future (2041-2070)	80	72 to 89
Absolute Anomalies (mm)	17	9 to 26
Percent Anomalies (%)	25	13 to 41
25-Year Return Period (mm)	Ensemble Average	Range (Min to Max)
Past (1971-2000)	75	62 to 77
Future (2041-2070)	96	81 to 113
Absolute Anomalies (mm)	21	4 to 39
Percent Anomalies (%)	28	1 to 60
Snow Proxy (events)	Ensemble Average	Range (Min to Max)
Past (1971-2000)	18	17 to 19
Future (2041-2070)	13	8 to 17
Absolute Anomalies (events)	-5	-10 to -1
Percent Anomalies (%)	-26	-55 to -8

Table 4: Projections of precipitation indicators from 10 downscaled regional climate models for Bear Pass Highway. The regionally averaged values are obtained from the spatial average of the cells within the 10km highway region boundary.

4.3. Pine Pass

The climate of Pine Pass is considerably different from that of either Bella Coola or Bear Pass, which is reflected in both the historical observations and the future projections. The largest precipitation amounts are received during the summer months and over the mountains in the middle of the highway section (Figure 13). As noted in the methods section, no weather station with sufficient data quality could be found along the highway section so a single ANUSPLIN grid cell near Mt. Lemoray in the middle of the pass was used as a substitute. This results in site values and regional averages that are much closer to each other than those of the other two regions. The Mt. Lemoray site experienced 682 mm of precipitation annually over 1951-2005 and recorded 5-day precipitation of 44 mm, a 10-year return period of 41 mm and a 25-year return period of 56 mm. These values are similar to the regional averages listed in **Error! Reference source not found.**

Indicator	Site Value (ANUSPLIN Cell)	ANUSPLIN Regional Value
Annual Total Precipitation (mm/year)	682	653
5-Day Total Precipitation (mm)	44	56
10-Year Return Period (mm/24 hrs)	41	35
25-Year Return Period (mm/24 hrs)	56	41
Snow Proxy (events/year)	9	4

Table 5: Precipitation indicators for Pine Pass highway from an ANUSPLIN grid cell (site) and regionally averaged ANUSPLIN (1951-2005) observations. The regionally averaged values are obtained from the spatial average of the cells within the 10km highway region boundary.

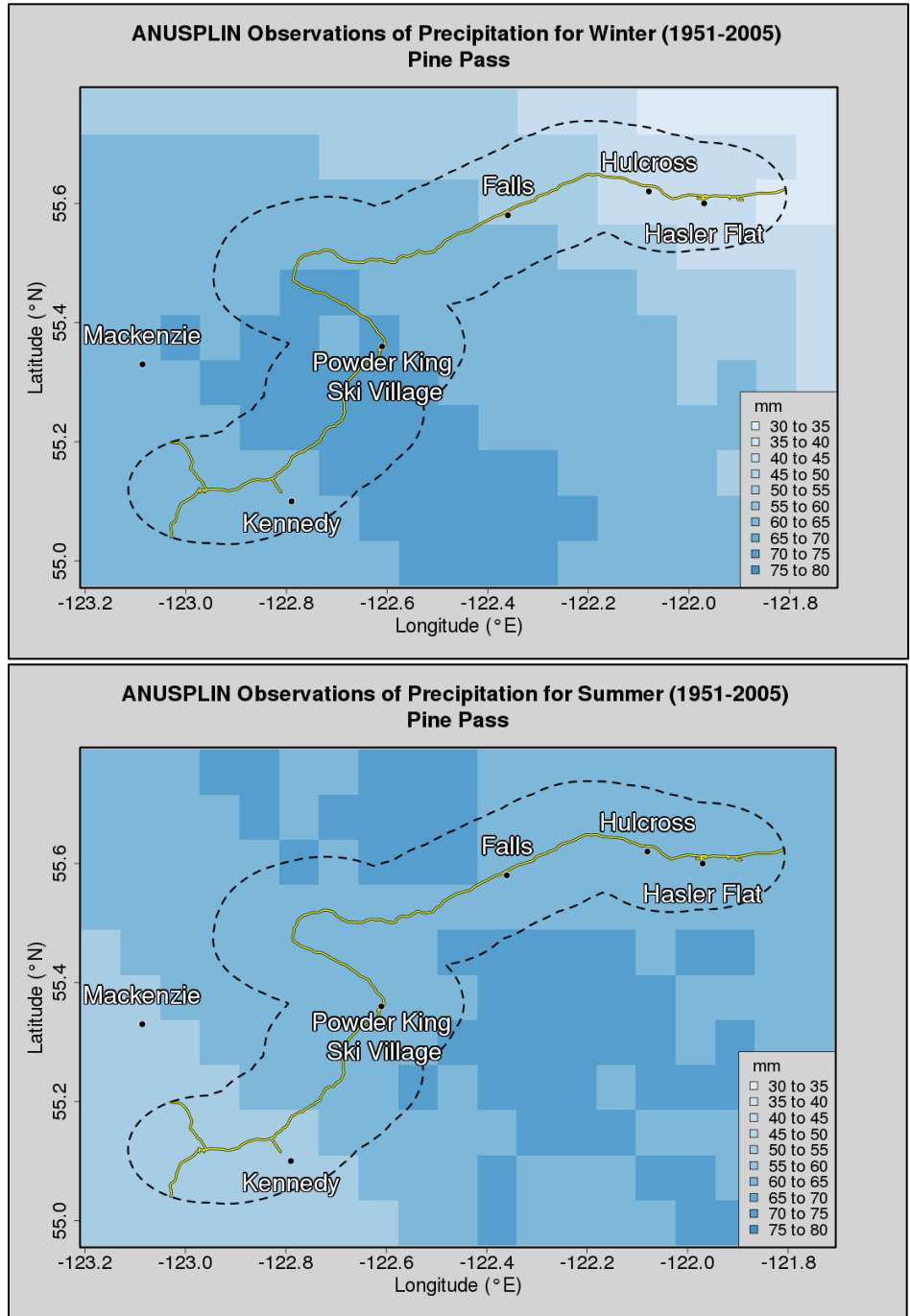


Figure 13: Winter (top) and summer (bottom) precipitation totals for the Pine Pass Highway (yellow line) obtained from the ANUSPLIN dataset and averaged over 1951-2005. The dashed line indicates the 10km highway region boundary.

Projected precipitation indicator increases in Pine Pass are less than those in the other regions with annual precipitation, 5-day precipitation totals and snow proxy are projected to increase by 11% to 12% (**Error! Reference source not found.**). The increases occur in both the fall and winter months as well as in June, with a notable shift in the largest

monthly precipitation amounts received from July to June by the 2050s. Spatially, the fall and winter percent increases are fairly uniform in their distribution over the highway section while the summer increases are largest over the eastern end of the highway moving towards Hasler Flat (Figure 14).

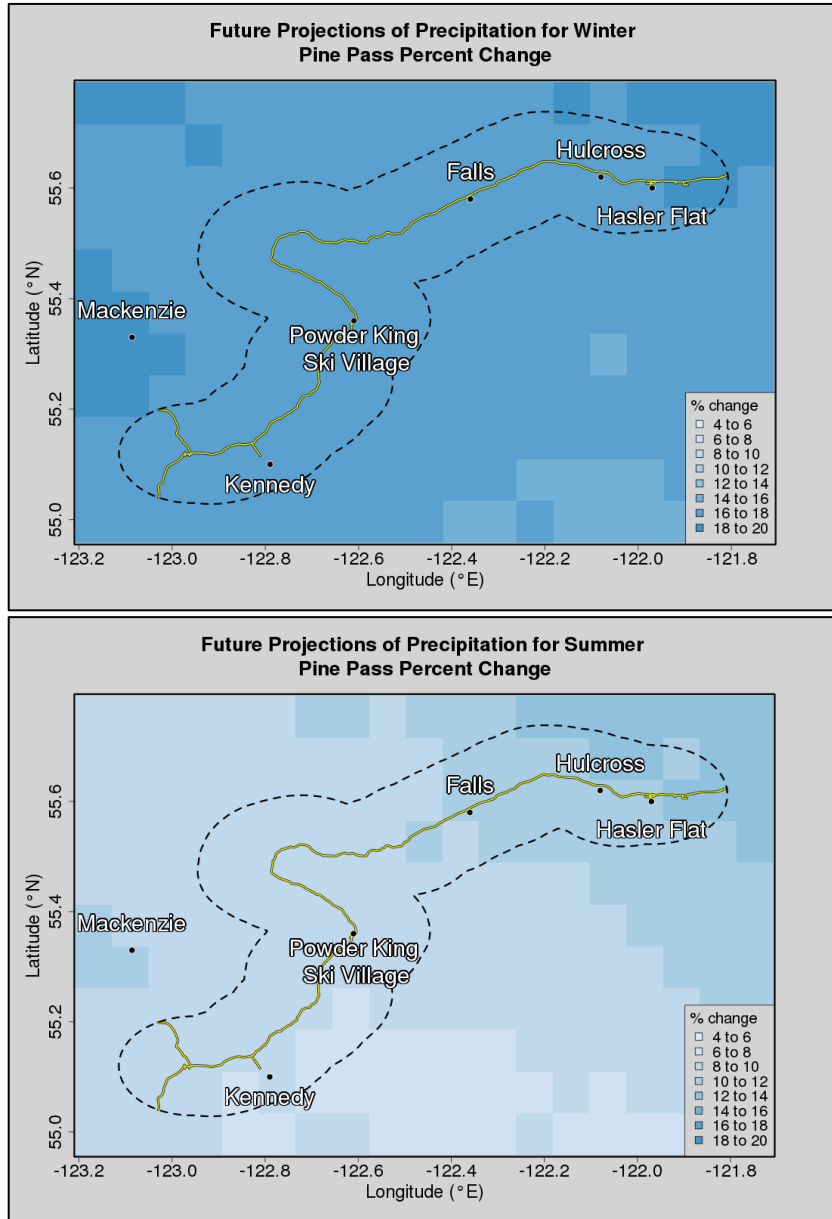


Figure 14: Projected 2050s (percent change) in winter (top) and summer (bottom) precipitation for the Pine Pass Highway (yellow line) obtained from an ensemble of 10 downscaled regional climate model simulations. The dashed line indicates the 10km highway region boundary.

Annual Total Precipitation (mm/year)	Ensemble Average	Range (Min to Max)
Past (1971-2000)	653	644 to 658
Future (2041-2070)	734	636 to 796
Absolute Anomalies (mm)	81	-18 to 144
Percent Anomalies (%)	12	-3 to 22
5-Day Precipitation (mm)	Ensemble Average	Range (Min to Max)
Past (1971-2000)	53	50 to 56
Future (2041-2070)	59	54 to 68
Absolute Anomalies (mm)	5	1 to 16
Percent Anomalies (%)	11	1 to 31
10-Year Return Period (mm)	Ensemble Average	Range (Min to Max)
Past (1971-2000)	35	33 to 36
Future (2041-2070)	42	35 to 57
Absolute Anomalies (mm)	7	1 to 23
Percent Anomalies (%)	21	2 to 69
25-Year Return Period (mm)	Ensemble Average	Range (Min to Max)
Past (1971-2000)	41	35 to 45
Future (2041-2070)	51	40 to 83
Absolute Anomalies (mm)	12	-1 to 44
Percent Anomalies (%)	24	-3 to 111
Snow Proxy (events)	Ensemble Average	Range (Min to Max)
Past (1971-2000)	3.8	3.3 to 4.4
Future (2041-2070)	4.2	2.6 to 5.8
Absolute Anomalies (events)	0.4	-1 to 1.9
Percent Anomalies (%)	11	-25 to 48

Table 6: Projections of precipitation indicators from 10 downscaled regional climate model simulations for Pine Pass Highway. The regionally averaged values are obtained from the spatial average of the cells within the 10km highway region boundary.

5. Discussion and Conclusions

Applying statistical downscaling to simulations of precipitation produces daily values that are closer to the observed patterns of precipitation in each of the three highway regions. By design, statistical downscaling adjusts large scale climate model simulations to match the statistics of gridded observations from ANUSPLIN as closely as possible. Higher resolution simulations are able to include more detailed features such as mountains and valleys that can strongly affect where and how much precipitation falls. Capturing the effect of these features on average and extreme precipitation is important when the area of study is small compared to the size of a global climate model grid cell as is the case for the highways.

Precipitation indicators at each of the three highway regions are projected to increase with larger increases (and larger ranges of projected change) in the more extreme indicators. Absolute anomalies are largest in the winter months, while the relative changes are larger in the summer season, as a result of lower historical precipitation during the summer months. Annual total precipitation is projected to increase between 11% at Bella Coola and 15% at Bear Pass by the 2050s (2041-2070) compared to the historical baseline of 1971-2000. Sustained precipitation, measured by the annual maximum 5-day total, is projected to increase between 11% at Pine Pass and 25% at Bear Pass. Less frequent 10-Year return period events are projected to increase between 15% at Pine Pass and 31% at Bella Coola over the same period. Snow proxy (used to estimate snowfall) is projected to decrease at Bear Pass and experience little change in the other regions, reflecting the competing effects of both increased precipitation and increased temperatures.

The ranges of projected change associated with each indicator span the minimum and maximum values from the 10 downscaled regional climate models. The ranges incorporate both the differences in future simulations when obtained using different climate models and contributions from sources of uncertainty. Uncertainty in the projections arises from elements such as sampling error in estimating parameter of the GEV distribution for the return periods or having only 30 years of observations to calculate the indicators. Using multiple regional climate models all following the same emissions scenario helps to reduce but not eliminate these sources of uncertainty.

In discussion with the MOTI working group, one of the issues identified was increased streamflow due to snowmelt driven peak flow events. This kind of event is a known potential cause of significant damage to infrastructure on each of the three highway sections. As modelled streamflow was not available for the regions of interest, short and medium duration precipitation events were used to characterize potential increase in the rainfall component and a snowfall proxy was used to estimate changes in snowfall. This information was combined with the local experience of engineers following the PIEVC protocols to assess the potential future risk from these events. More detailed studies of streamflow, runoff and other hydrological parameters would require hydrologic modelling, such as the work performed by the Hydrologic Group at PCIC (Schnorbus, Werner, & Bennett, 2014).

The analysis and projections produced for this study were made using the methods and data available at the time of the project. For example, atmospheric rivers are not considered separately in this analysis but were included in the broader analysis of short and long duration extreme precipitation. Current research into atmosphere river events specifically, and atmospheric circulation more generally, will address questions on current conditions and projected changes in these types of events. Research in climate modelling and analysis is ongoing, with new data and methods becoming available as resources allow.

6. References

- Cannon, A. J., Sobie, S. R., & Murdock, T. Q. (In Prep). Downscaling Extremes - an intercomparison of multiple gridded methods. *In Prep*.
- Dettinger, M. D., Ralph, F. M., Das, T., Neiman, P. J., & Cayan, D. R. (2011). Atmospheric Rivers, Floods and the Water Resources of California. *Water*, 3(2), 445–478. doi:10.3390/w3020445
- Hunter, R. D., & Meentemeyer, R. K. (2005). Climatologically Aided Mapping of Daily Precipitation and Temperature. *Journal of Applied Meteorology*, 44(10), 1501–1510. doi:10.1175/JAM2295.1
- Lapp, D. (2013). Infrastructure Climate Risk Assessment Backgrounder. Engineers Canada.
- McKenney, D. W., Hutchinson, M. F., Papadopol, P., Lawrence, K., Pedlar, J., Campbell, K., ... Owen, T. (2011). Customized Spatial Climate Models for North America. *Bulletin of the American Meteorological Society*, 92(12), 1611–1622. doi:10.1175/2011BAMS3132.1
- Mearns, L. O., Gutowski, W., Jones, R., Leung, R., McGinnis, S., Nunes, A., & Qian, Y. (2009). A Regional Climate Change Assessment Program for North America. *Eos, Transactions American Geophysical Union*, 90(36), 311–311. doi:10.1029/2009EO360002
- Moore, R. D., Spittlehouse, D. L., Whitfield, P., & Stahl, K. (2010). Weather and Climate. In *Compendium of forest hydrology and geomorphology in British Columbia* (Vols. 1-19, Vol. 3).
- Murdock, T. Q., & Spittlehouse, D. L. (2011). *Selecting and Using Climate Change Scenarios for British Columbia*. University of Victoria.

- Nakićenović, N. (2000). Special Report on Emissions Scenarios. *Special Report on Emissions Scenarios*, 599.
- Nodelman, J. (2010, June 2). Climate Change Engineering Vulnerability Assessment - Coquihalla Highway (B.C. Highway 5) Between Nicolum River and Dry Gulch. Nodelcorp.
- Nodelman, J. (2013, September 30). Climate Change Engineering Vulnerability Assessment of Three British Columbia Highway Segments. Nodelcorp.
- Schnorbus, M., Werner, A., & Bennett, K. (2014). Impacts of climate change in three hydrologic regimes in British Columbia, Canada. *Hydrological Processes*, 28(3), 1170–1189. doi:10.1002/hyp.9661
- Zwiers, F. W., Alexander, L. V., Hegerl, G. C., Knutson, T. R., Kossin, J. P., Naveau, P., ... Zhang, X. (2013). Climate Extremes: Challenges in Estimating and Understanding Recent Changes in the Frequency and Intensity of Extreme Climate and Weather Events. In G. R. Asrar & J. W. Hurrell (Eds.), *Climate Science for Serving Society* (pp. 339–389). Springer Netherlands. Retrieved from http://link.springer.com/chapter/10.1007/978-94-007-6692-1_13